JOURNAL OF RAMAN SPECTROSCOPY
J. Raman Spectrosc. 2008; **39**: 793–805
Published online 22 February 2008 in Wiley InterScience
(www.interscience.wiley.com) DOI: 10.1002/jrs.1912

JRS

Ionic liquid structure: the conformational isomerism in 1-butyl-3-methyl-imidazolium tetrafluoroborate ([bmim][BF_4])

R. Holomb,[1]*,† A. Martinelli,[1] I. Albinsson,[2] J. C. Lassègues,[3] P. Johansson[1] and P. Jacobsson[1]

[1] Department of Applied Physics, Chalmers University of Technology, Göteborg, SE-412 96, Sweden
[2] Department of Physics, Göteborg University, Göteborg, SE-412 96, Sweden
[3] Laboratoire de Physico-Chimie Moléculaire, UMR 5803, CNRS, Université Bordeaux I 351 Cours de la Libération, 33405 Talence Cedex, France

Received 9 August 2007; Accepted 1 December 2007

As a probe of local structure, the vibrational properties of the 1-butyl-3-methylimidazolium tetrafluoroborate [bmim][BF_4] ionic liquid were studied by infrared (IR), Raman spectroscopy, and *ab initio* calculations. The coexistence of at least four [bmim]$^+$ conformers (GG, GA, TA, and AA) at room temperature was established through unique spectral responses. The Raman modes characteristic of the two most stable [bmim]$^+$ conformers, GA and AA, according to the *ab initio* calculations, increase in intensity with decreasing temperature. To assess the total spectral behavior of the ionic liquid both the contributions of different [bmim]$^+$ conformers and the [bmim]$^+$— [BF_4]$^-$ interactions to the vibrational spectra are discussed. Copyright © 2008 John Wiley & Sons, Ltd.

Supplementary electronic material for this paper is available in Wiley InterScience at http://www.interscience.wiley.com/jpages/0377-0486/suppmat/

KEYWORDS: ionic liquids; 1-butyl-3-methyl-imidazolium; $bmim^+$; BF_4^-; conformers; IR spectroscopy; Raman spectroscopy; *ab initio* calculations

INTRODUCTION

Ionic liquids (ILs) composed of organic cations and inorganic anions is a class of salts that remain liquid at room temperature.[1] Several unique physicochemical properties in combination such as nonvolatility, inflammability, thermal stability, recyclability, and good solvating capabilities indicate that ILs can be useful materials for applications in separation,[2] catalysis,[3] electrochemistry,[4] etc. The wide liquidus range, high heat capacity, and density allow them to be used as thermal and heat transfer media.[5] In addition, the high ionic conductivity and electrochemical stability make ILs excellent candidates for electrolytes avoiding corrosion, leakage, volatility, and flammability.[6,7]

Investigations of fundamental physicochemical properties of ILs composed by different cations and anions should provide a deeper understanding of structural features and the role of molecular interactions in ILs. Over the large range of possible cation and anion variations in ILs, the imidazolium-based ILs are the most studied today both experimentally and computationally. Especially, the molecular level structure has been in focus in many of the studies. For example, by using *ab initio* methods Turner *et al*.[8] have found two local energy minima for the 1-ethyl-3-methylimidazolium cation, $emim^+$ a.k.a. EMI, corresponding to the more stable nonplanar (*np*) and less stable planar (*p*) forms. Similarly, through combining Raman spectroscopy of different [emim]$^+$ salts and *ab initio* calculations, Umebayashi *et al*.[9] showed the presence of these [emim]$^+$ conformers and evaluated their population in the [emim][BF_4] IL to be 0.61 and 0.39 for *np* and *p* [emim]$^+$ forms, respectively. In a recent study, the population of *np* [emim]$^+$ cations in the [emim][TFSI] IL was found to be 87% at room temperature.[10] By using X-ray crystallographic and Raman studies, Hayashi *et al*.[11] found two polymorphs of crystalline 1-butyl-3-methylimidazolium chloride, [bmim][Cl], with the local structures both existing also in the liquid state. Holbrey *et al*.[12] reported similarity between the structure of [bmim]$^+$ in [bmim][Br] and in one of the [bmim][Cl] polymorphs.

The longer alkyl chain length compared to [emim]$^+$ allows [bmim]$^+$ to have additional conformation states:

*Correspondence to: R. Holomb, Department of Applied Physics, Chalmers University of Technology, Göteborg, SE-412 96, Sweden.
E-mail: romhol@fy.chalmers.se
†On leave from the Institute for Solid State Physics and Chemistry, Uzhhorod National University, Uzhhorod, Ukraine.

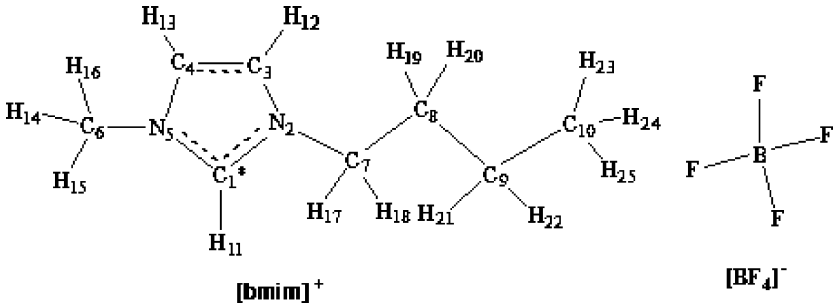

Figure 1. The chemical structures of the cation and anion components of [bmim][BF_4].

combinations of gauche (G) and anti (A). For $[emim]^+$, the conformers (*p* and *np*) are obtained by rotation about the N_2-C_7 bond (Fig. 1). For $[bmim]^+$ these states can be combined with rotations around both C_7-C_8 and C_8-C_9 bonds. While all such conformers have not yet been found in the crystalline state, their presence in the liquid state of ILs can obviously be reasoned and measured spectroscopically. Ozawa *et al*. were the first to show the contributions of different $[bmim]^+$ conformers to the Raman spectra of the [bmim][BF_4] ionic liquid.[11,13] In addition, Berg *et al*.[14] found that the Raman bands characteristic for the GA and AA $[bmim]^+$ conformers are also characteristic for the 1-hexyl-3-methylimidazolium cation, $[hmim]^+$. The differences in concentration of G and A (C_7-C_8) $[bmim]^+$ conformers in molten [bmim][Cl], [bmim][Br], and liquid [bmim][I] were clearly detected by Raman spectroscopy.[15] A larger contribution of A conformations in [bmim][I] compared to molten [bmim][Cl], [bmim][Br], and the coexistence of two conformers of $[bmim]^+$ were suggested to be responsible for the low melting point of [bmim][I]. However, using *ab initio* calculations of different cation–anion pairs Heimer *et al*.[16] have detected only a minimal effect of alkyl chain conformations on the vibrational spectra of several methyl-imidazolium based ILs, [C_{2-4}mim][BF_4]. In a recent study, Katsyuba *et al*.[17] have shown that the concentration of different conformers may depend on the type and position of the anion and, therefore, the vibrations of the cations depend both on the conformations and on the cation–anion association. Katsyuba *et al*. also proposed a model considering isolated ion pairs as anharmonic oscillators to correlate with the melting points of ILs.

However, none of these studies have made any definite statements about all the $[bmim]^+$ cation conformers possibly present and how to unambiguously detect them, including the role of Coulombic and hydrogen bond interactions. We believe that the combined usage of spectroscopic studies and *ab initio* calculations is the most powerful tool to resolve this issue in detail. As mentioned the conformers of $[emim]^+$ have already been analyzed and identified.[9,10] $[bmim]^+$, on the other hand, has many more possible conformers, allowing more statistical significant results, while still being small enough to allow the IR and Raman spectra of all conformers to be calculated *ab initio* with some appreciable accuracy. It will therefore serve as an excellent probe for the viability of the approach in general. Therefore, this article is aimed at *ab initio* studies of the vibrational properties of $[bmim]^+$ conformers and $[bmim]^+ - [BF_4]^-$ pair models. The computational results are subsequently compared with IR and Raman spectroscopy data. From the data, a picture is created of the local structure of the [bmim][BF_4] ionic liquid, a picture that should be partly transferable to imidazolium-based ILs in general.

MATERIALS AND METHODS

The [emim][BF_4] and [bmim][BF_4] ILs were purchased from Merck.[18] The liquidus range and the glass transition temperature (T_g) of [bmim][BF_4] was determined by calorimetric measurements performed on a differential scanning calorimeter (Mettler DSC30) with a TC10A/TC15 control system and STARe Software version 8.10. The sample was sealed in an aluminum crucible under inert atmosphere. The sample was scanned in three steps; first upwards to 363 K, then down to 123 K, and finally upwards to 363 K again, with a scanning rate of 10 K/min.

Room temperature attenuated total reflectance (ATR)-IR spectra were measured in an Ar-filled dry box using a Bruker Vector 22 Fourier transform infrared (FTIR) spectrometer and a Golden Gate Mk II single reflection diamond ATR unit (Specac). The ATR FTIR spectra presented here has not been corrected for the penetration depth and the dispersion functions. For the Raman measurements, quartz cuvettes were sealed under Ar inside the dry box. Room temperature FT-Raman spectra were measured in back-scattering geometry using a Bruker IFS 66 interferometer with a liquid nitrogen cooled Ge-detector coupled to a Bruker FRA 106 Raman module. A near-IR Nd:YAG laser with a wavelength of 1064 nm was used as the excitation source. The temperature-dependent Raman spectra of [bmim][BF_4] were measured using a Dilor-XY800 spectrometer with a CCD camera cooled by liquid nitrogen. An Ar/Kr laser with a wavelength of 514.5 nm was used as the excitation source. For the low-temperature studies the sample was placed inside a cryostat. For each measurement temperature, the sample was

DOI: 10.1002/jrs

equilibrated for at least 30 min before the spectra were measured. The spectral resolution of all measurements was $\sim 2\ cm^{-1}$.

The computational part of the studies consisted of first-principle calculations of geometries, total energies, atomic charges, and vibrational properties of the $[BF_4]^-$ anion, the $[bmim]^+$ cation conformers, and $[bmim]^+ - [BF_4]^-$ pair models. In order to further study the influence of the ion-pair interaction on the anion structure, a C_{3v} symmetry $[Li]^+ - [BF_4]^-$ pair was used. The initial structures of the $[bmim]^+$ cation conformers were obtained by combined rotations of the CH_2 groups of the $C_7–C_8$ and $C_8–C_9$ bonds. This way, the $G^{+/-}G^{+/-}$, $G^{+(-)}A$, $AG^{+(-)}$, and AA conformers were obtained and thereafter denoted as GG, GA, AG, and AA (Fig. 2(a)–(d)). Several of these conformers are structurally and spectroscopically very similar, but at least five different $[bmim]^+$ conformers converge to different local energy minima. However, only four of them are important for modeling the real ionic liquid; the totally planar AA $[bmim]^+$ conformer (similar to the *p* form of $[emim]^+$ and not presented here) was excluded from further analysis as long chain planarity hardly can be observed in the liquid state, a clear difference between gas phase (calculated) *versus* liquid phase (expected) preference. This is supported by that, in spite of being a low energy conformer, the simulated IR and Raman spectra of this conformer strongly disagree with the experimental spectra of $[bmim][BF_4]$.

In order to study the influence of $[bmim]^+$ – anion interactions on the vibrational spectra, simple cation–anion pair models based on the GA conformer were used. The two 'closed' and 'open' cation–anion pair models differ in the position of $[BF_4]^-$ and in the direction of the alkyl chain (Fig. 2(e)–(f)). In the 'open' model, the anion is placed on the opposite side of the imidazolium ring plane with respect to the alkyl chain. This allows the anion to interact predominantly with the cation ring, whereas in the 'closed' model the alkyl chain is closer and anion interaction both with the ring and chain is obtained.

All calculations were performed using the Gaussian-03 quantum-chemical package.[19] The DFT method using the hybrid B3LYP functional consisting of a linear combination of the pure corrected exchange functional by Becke[20] and the three-parameter gradient-corrected correlation functional by Lee *et al*.[21] was applied for geometry optimizations and IR and Raman spectra calculations. The triple zeta valence (TZV) Pople 6-311+G* basis set was used for all atoms.[22] The Breneman and Wiberg *CHELPG* scheme[23,24] was used to determine atomic charges from electrostatic potentials. To simulate spectra from the computed IR and Raman data, Lorentz functions were applied for each of the computed modes using full width at half-height (FWHH) parameters of 20 and 10 cm^{-1} for the IR and Raman spectra, respectively.

RESULTS AND DISCUSSION

Basic structural aspects

Structural models and overall vibrational properties of [bmim][BF4]

Structural properties are the basis for understanding the vibrational, thermodynamic, and other properties of ILs. Coulombic, van der Waals, and hydrogen bonding effects can all take place in ILs and determine the ILs structural and physicochemical properties and can also influence and thus be detected in their vibrational spectra. As an example, the existence of hydrogen bonds has been found computationally and spectroscopically in different ILs.[8,25–29] At the same time, experimental and computational results together show the considerable influence of cation and anion conformations on the vibrational spectra of imidazolium-based ILs.[9–15] It is thus necessary to elucidate the unique effect of all possible mechanisms on the resulting IL spectra. While the cation–cation interactions are important with respect to the creation of extended local structures in ILs, increasing with increasing alkyl chain length,[15,30] the nature of these interactions are still unclear and not likely to significantly affect the intermolecular vibrations of the cations. Therefore, we find a single cation model to be appropriate for the conformational isomerism.

Measured room temperature IR spectra of the [bmim][BF_4] and [emim][BF_4] ILs are shown in Fig. 3(a). The C–H stretching vibrations of the methyl and methylene groups occur below $\sim 3050\ cm^{-1}$ and the ring C–H stretching vibrations occur above $\sim 3050\ cm^{-1}$. Consequently, the IR profiles of both ILs are very similar above $\sim 3050\ cm^{-1}$, but they differ below as expected from the presence of two additional methylene groups in $[bmim]^+$. The other significant difference found in the IR spectra is at *ca* 700 cm^{-1}. This band originates from alkyl groups connected to the ring N atoms in both *p* and *np* $[emim]^+$ conformers.

Figure 3(b) shows the corresponding Raman spectra and the observed differences in the C–H stretching region remain. Other interesting features are found in the spectral region 200–1200 cm^{-1}. These differing features are presumably related with the two additional methylene groups of the $[bmim]^+$ cation and can therefore be used to identify different $[bmim]^+$ conformers. Especially, in the region most sensitive to conformational changes, 800–1000 cm^{-1}, at least four new modes with peak positions at 808, 825, 883, and 905 cm^{-1} are observable in the Raman spectra of $[bmim][BF_4]$ – in a spectral region almost empty for $[emim][BF_4]$. In addition, new features are observed at 325, 623, 976, 1055, and 1116 cm^{-1}.

Thus, while IR spectroscopy is almost insensitive to $[bmim]^+$ conformational changes, Raman spectroscopy can be extremely useful for identification of different $[bmim]^+$ conformers.

Geometries and energies

The optimized geometries of the $[bmim]^+$ cation conformers, the $[bmim]^+ - [BF_4]^-$ ion pair models and the values of

DOI: 10.1002/jrs

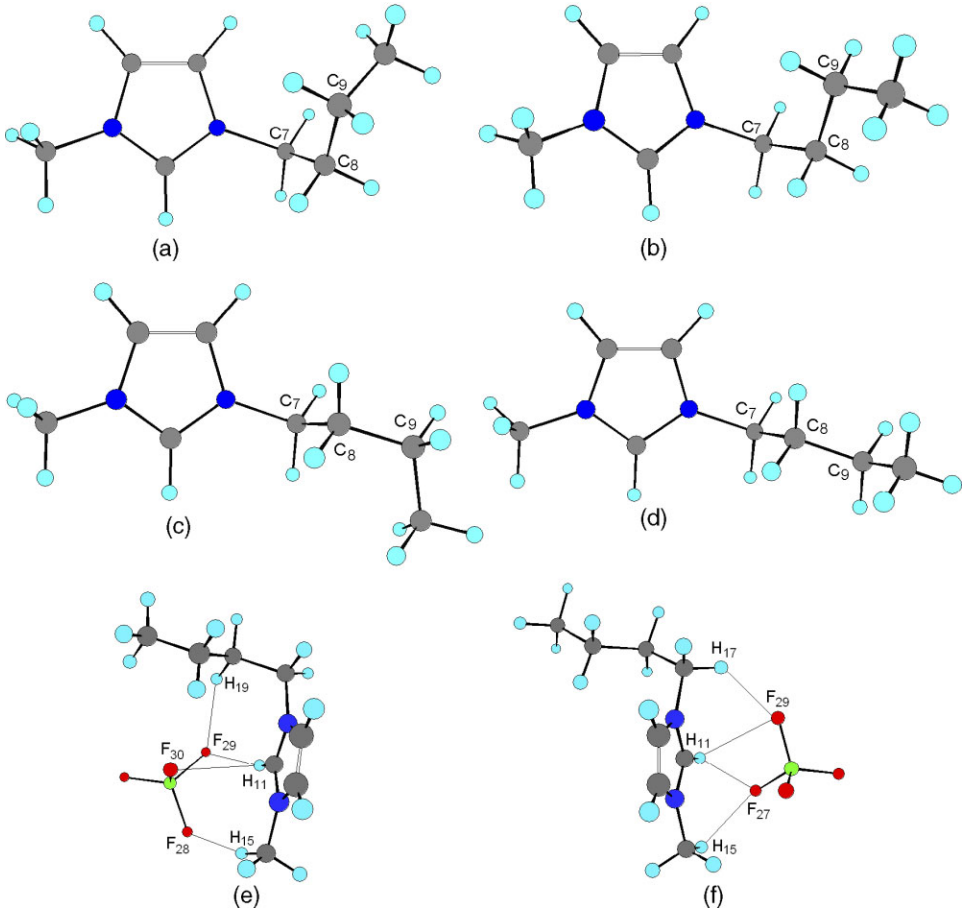

Figure 2. Optimized geometry of GG (a), GA (b), AG (c), AA (d) $[bmim]^+$ conformers and $[bmim(GA)]^+ - [BF_4]^-$ 'closed' (e) and 'open' (f) pair models. H-bond distances (Å): (e) 1.95 (F_{29}–H_{11}), 2.08 (F_{28}–H_{15}), 2.37 (F_{29}–H_{19}), 2.54 (F_{30}–H_{11}); (f) 2.01 (F_{27}–H_{11}), 2.27 (F_{29}–H_{17}), 2.38 (F_{29}–H_{11}), 2.45 (F_{27}–H_{15}). This figure is available in colour online at www.interscience.wiley.com/journal/jrs.

Table 1. Total energies (E^{tot}) and dipole moments ($|\vec{P}|$) of $[BF_4]^-$ anion, $[bmim]^+$ conformers, and $[bmim(GA)]^+ - [BF_4]^-$ cation–anion pairs. The binding energies of $[bmim(GA)]^+ - [BF_4]^-$ ion pairs relative to free $[BF_4]^-$ anion and $[bmim(GA)]^+$ cation are shown in the last string ($\Delta E_{bind} = E^{tot}_{[bmim(GA)]^+-[BF4]^-} - \left[E^{tot}_{[bmim(GA)]^+} + E^{tot}_{[BF4]^-}\right]$)

Structure / Property	$[bmim]^+$ conformers				$[BF_4]^-$ (T_d symmetry)	$\frac{[bmim(GA)]^+-[BF_4]^-}{([emim(np)]^+-[BF_4]^-)}$	
	AA	GA	AG	GG		'open'	'closed'
E^{tot}, a. u.	−423.2667	−423.2658	−423.2655	−423.2645	−424.6797	−848.0771	−848.0773
ΔE^{tot}, kJ mol^{-1}	0.00	2.36	3.15	5.78	–		
$\|\vec{P}\|$, Debye	5.76	4.96	5.30	4.78	–	13.06	13.09
ΔE_{bind}, kJ mol^{-1}						$\frac{-345.6}{(-348.2)}$	$\frac{-346.0}{(-350.3)}$

the shortest F···H distances (i.e. H-bonds) are schematically shown in Fig. 2.

The total energies and energy differences between $[bmim]^+$ conformers and their dipole moments are found in Table 1. According to the calculations, the AA conformer has the lowest energy. The next three $[bmim]^+$ conformers are +2.36, +3.15, and +5.78 kJ mol^{-1} for GA, AG, and GG, respectively. For comparison, using the same computational level, the energy difference between the *p* and *np* $[emim]^+$ conformers was +2.12 kJ mol^{-1}. It is important to note that the difference in energy between cation conformers is only on the order of the thermal energy (kT = 2.48 kJ mol^{-1}) at room temperature. Therefore, all of these conformers are likely to coexist in the liquid state.

DOI: 10.1002/jrs

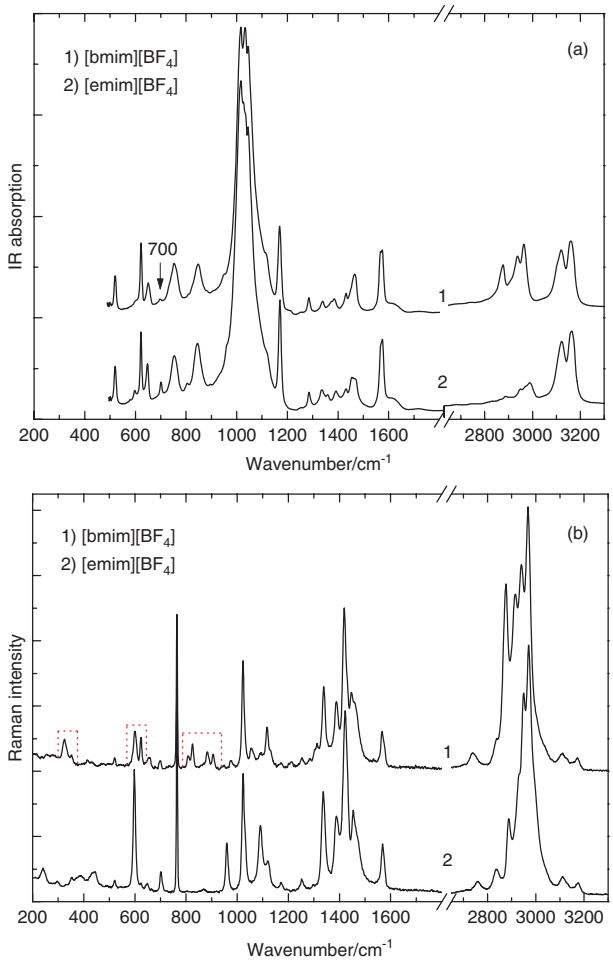

Figure 3. IR (a) and Raman (b) spectra of 1-butyl-3-methyl-imidazolium (curves 1) and 1-ethyl-3-methyl-imidazolium (curves 2) tetrafluoroborate ionic liquids. Selected spectral regions in the Raman spectra of [bmim][BF_4] show the main differences compared to the spectra of [emim][BF_4] (The Raman intensities of high frequency C–H stretching vibrations are divided by a factor 2). This figure is available in colour online at www.interscience.wiley.com/journal/jrs.

The ion-pair calculations indicate that the binding energies of 'closed' and 'open' models are quite large, very similar, and somewhat lower than for the $[emim]^+ - [BF_4]^-$ pairs, indicating the lower ion pairing probability for an increasing alkyl chain length of the imidazolium cation. However, as shown in,[8,27,31] both the position and type of anion have a significant influence. The optimal geometry of $[BF_4]^-$ anions in pair models differs both from the gas phase (T_d) and from the C_{3v} symmetry found in a $[Li]^+ - [BF_4]^-$ pair. For the gas phase T_d geometry, B–F bond distances of 1.42 Å were obtained. For the $[Li]^+ - [BF_4]^-$ model, the optimized B–F distances were 1.34 and 1.45 Å and the F–B–F angles were 102.3 and 116.0°. The B–F bond distances in 'open' and 'closed' pair models ranged from 1.37 to 1.44 Å and from 1.38 to 1.44 Å, respectively. The corresponding F–B–F angles are in the ranges of 107.0–112.1° and 106.6–112.3° for 'open' and 'closed' pairs, respectively.

Atomic charge distribution

Atomic charges of the $[bmim]^+$ cation conformers and $[bmim(GA)]^+ - [BF_4]^-$ ion pairs are compiled in Table 2. The positive charge of the imidazolium ring indicates a predominant anion interaction site. A further analysis of the atomic charges explains why the anion is located around C_1H_{11} rather than C_3H_{12} or C_4H_{13}; most of the positive charge is concentrated on the $N_2C_1(H_{11})N_5$ subgroup.[32] The main differences in atomic charge distribution between conformers are observed between the GG, GA, and AG conformers and the AA conformer. The more positive charge of the imidazolium ring in AA is entirely due to the increased positive charge on the N_2 atom. The first methylene group of AA is approximately uncharged, due to the negative charge of the C_7 atom, while positive for all other $[bmim]^+$ conformers. On the contrary, the second CH_2 group of AA is positively charged (due to the positive charge of C_8) while a total charge closer to neutral was calculated for this group in GG, GA, and AG conformers. These charge differences may have profound effects on the vibrational spectra of the different conformers and the anion arrangement in the cation–anion pairs.

The atomic charge distribution of the $[bmim(GA)]^+ - [BF_4]^-$ ion pairs and the $[bmim(GA)]^+$ cation differs both in the imidazolium ring part and in all methylene groups. The largest differences for the ring were observed for 'open' pair model where the positive charge of both N atoms increases. There are also large differences in the charges of the second CH_2 groups: charge differences of −0.09 and +0.20 were calculated for the C_8 atom of 'open' and 'closed' models, respectively. Also these charge differences may be important when elucidating the role of the different ion pairs to the observed vibrational spectra.

Detailed IR spectroscopy study

The 400–1600 cm^{-1} region

The calculated wavenumbers of $[BF_4]^-$ in T_d symmetry together with the IR and Raman intensities are compiled in Table 3. The calculated vibrational modes of the C_{3v} $[Li]^+ - [BF_4]^-$ pair with a strong and directional interaction and nonsymmetric $[BF_4]^-$ in $[bmim(GA)]^+ - [BF_4]^-$ pairs are also shown for comparison. The calculated IR spectra of all four $[bmim]^+$ conformers are shown together with the experimental spectrum of the [bmim][BF_4] IL in Fig. 4(a). The calculated IR spectrum for each of the $[bmim]^+$ conformers agrees well with the experimental spectrum and only very small differences among the $[bmim]^+$ conformers are found. The main difference is the redistribution of mode intensities at 624 and 653 cm^{-1}. The band at 624 cm^{-1} can be assigned to a mixture of out-of-plane ring bending and in-phase $CH_2(N)$ and $CH_3(N)$ CN stretching vibrations (Table 4). This band is,

Table 2. Atomic charges of the $[bmim]^+$ conformers calculated using *CHELPG* scheme. Values in brackets indicate the total charges of the groups

		$[bmim]^+$				$[bmim(GA)]^+ - [BF_4]^-$	
Group/Atom		GG	AG	AA	GA	'open'	'closed'
CH_3 (at ring)	C_6	−0.25	−0.22	−0.19	−0.21	−0.24	−0.20
	H_{14}	0.15	0.14	0.13	0.14	0.09	0.12
	H_{15}	0.14	0.13	0.13	0.13	0.16	0.18
	H_{16}	0.15	0.14	0.13	0.14	0.16	0.08
	(Tot.)	(0.19)	(0.19)	(0.20)	(0.20)	(0.16)	(0.18)
Imidazolium ring	$C_1{}^*$	−0.08	−0.08	−0.11	−0.05	−0.14	0.01
	H_{11}	0.22	0.21	0.22	0.21	0.24	0.19
	N_2	0.07	0.08	0.21	0.09	0.27	0.12
	C_3	−0.10	−0.13	−0.21	−0.13	−0.22	−0.23
	H_{12}	0.20	0.22	0.24	0.20	0.19	0.20
	C_4	−0.14	−0.14	−0.10	−0.11	−0.13	−0.10
	H_{13}	0.20	0.20	0.20	0.20	0.17	0.17
	N_5	0.17	0.17	0.14	0.13	0.20	0.13
	(Tot.)	(0.53)	(0.53)	(0.60)	(0.54)	(0.58)	(0.48)
CH_2 (I^{st})	C_7	0.03	−0.01	−0.23	−0.08	−0.15	−0.14
	H_{17}	0.06	0.07	0.12	0.09	0.14	0.08
	H_{18}	0.06	0.08	0.11	0.09	0.08	0.07
	(Tot.)	(0.15)	(0.14)	(−0.01)	(0.10)	(0.07)	(0.01)
CH_2 (II^{nd})	C_8	0.03	0.06	0.15	0.08	−0.01	0.28
	H_{19}	0.04	−0.01	−0.02	0.03	0.01	−0.02
	H_{20}	−0.02	0.00	−0.02	−0.01	0.04	−0.05
	(Tot.)	(0.05)	(0.05)	(0.11)	(0.09)	(0.04)	(0.20)
CH_2 (III^{d})	C_9	0.19	0.14	0.19	0.20	0.26	0.13
	H_{21}	−0.06	−0.01	−0.02	−0.05	−0.05	−0.06
	H_{22}	0.00	0.00	−0.02	−0.02	−0.10	0.00
	(Tot.)	(0.13)	(0.13)	(0.15)	(0.12)	(0.12)	(0.07)
CH_3 (end)	C_{10}	−0.25	−0.21	−0.28	−0.29	−0.23	−0.24
	H_{23}	0.08	0.05	0.09	0.07	0.06	0.06
	H_{24}	0.05	0.08	0.07	0.09	0.06	0.07
	H_{25}	0.07	0.04	0.07	0.08	0.04	0.04
	(Tot.)	(−0.05)	(−0.04)	(−0.05)	(−0.05)	(−0.07)	(−0.06)
BF_4	B					1.10	1.10
	F_{27}					−0.51	−0.47
	F_{28}					−0.47	−0.51
	F_{29}					−0.51	−0.49
	F_{30}					−0.51	−0.50
	(Tot.)					(−0.90)	(−0.87)

from the calculations, found to be more intense for AG and AA conformers. The band at 653 cm^{-1} represents a mixture of out-of-plane ring bending and CH_3(N) CN stretching vibrations. A small feature at ~697 cm^{-1} can be assigned to the GG and GA conformers and a mix of out-of-phase CH_2(N) and CH_3(N) CN stretching.

The most intense broad band with split peak positions at ~1015, ~1033, and ~1045 cm^{-1} is due to B–F stretching vibrations of $[BF_4]^-$ anions. Only one asymmetric B–F stretching (T_2 mode) at 1031 cm^{-1} exists for the tetrahedral (T_d) anion (Table 3), indicating that interactions in the IL result in distorted symmetry of $[BF_4]^-$ or a symmetric $[BF_4]^-$ in several environments. The former can be evaluated by use of the cation–anion pair models. Using the $[Li]^+ - [BF_4]^-$ model, the degeneracy is partially removed and hence two asymmetric B–F stretches ($E + A_1$ modes) are found at 924 and 1312 cm^{-1} (Table 3). Therefore, the large deviation in wavenumbers of asymmetric B–F stretching vibrations

DOI: 10.1002/jrs

Table 3. The computed mode wavenumbers and the corresponding IR and Raman intensities of $[BF_4]^-$ (T_d symmetry), $[BF_4]^-$ in $[Li]^+ - [BF_4]^-$ (C_{3v} symmetry), and nonsymmetric $[BF_4]^-$ in ion pairs

ν, cm^{-1}		I^{IR}, Km/Mole	I^R, $Å^4$/a.m.u.
$[BF_4]^-$ (T_d)			
337 (E)	ν_2	–	0.5
498 (T_2)	ν_4	2.8	0.8
734 (A_1)	ν_1	–	3.2
1031 (T_2)	ν_3	466.5	0.3
$[Li]^+ - [BF_4]^-$ (C_{3v})			
347 (E)	ν_2	0.2	0.4
503 (E)	ν_4	2.4	0.7
554 (A_1)	ν_4	12.2	0.8
740 (A_1)	ν_1	8.2	4.5
924 (E)	ν_3	447.5	0.1
1312 (A_1)	ν_3	417	0.1
$[bmim(GA)]^+ - [BF_4]^-$ ('open')			
343 (A)	ν_2	0.2	0.3
345 (A)	ν_2	0.1	0.3
497 (A)	ν_4	1.6	0.5
499 (A)	ν_4	3.4	0.6
508 (A)	ν_4	20.6	0.8
735 (A)	ν_1	9.5	3.4
954 (A)	ν_3	252.2	0.3
995 (A)	ν_3	281.3	0.6
1156 (A)	ν_3	425.9	1.4
$[bmim(GA)]^+ - [BF_4]^-$ ('closed')			
343 (A)	ν_2	0.1	0.3
350 (A)	ν_2	1.1	0.4
497 (A)	ν_4	1.7	0.4
500 (A)	ν_4	2.2	0.7
509 (A)	ν_4	14.5	0.4
737 (A)	ν_1	8.4	3.4
961 (A)	ν_3	155.1	0.4
1002 (A)	ν_3	302.1	0.3
1151 (A)	ν_3	482.1	0.6

around 1031 cm^{-1} can be a useful indicator of ion pairing in ILs. Furthermore, the complex atomic charge distribution in $[bmim]^+$ and H-bond interactions result in nonsymmetrical geometry (all degeneracy is removed) of $[BF_4]^-$ anions in $[bmim]^+ - [BF_4]^-$ pair models. However, the 3D-probability distribution of C_1^* atoms in $[bmim]^+$ cations around a $[PF_6]^-$ anion obtained from molecular dynamics (MD) simulations show a symmetrical character.[33] If it is also true for our system, the symmetrical surrounding of anions in [bmim][BF_4] can keep most $[BF_4]^-$ in T_d symmetry. Figure 4(b) shows the calculated IR spectra of 'open' and 'closed' $[bmim(GA)]^+ - [BF_4]^-$ pairs. The strong interactions in these models (Table 1) should result in significant shifts of the asymmetric B–F stretching vibrational modes. A similar effect was found by Katsyuba *et al.*[34] for $[emim]^+ - [BF_4]^-$ ion pairs. Three IR modes at 954, 995, and 1156 cm^{-1} and at 961, 1002, and 1151 cm^{-1} were calculated for 'open' and 'closed' pairs, respectively. The modes at 954 and 961 cm^{-1} are assigned to mixtures of B–F stretching and out-of-plane NC(H)N CH bending vibrations. The broad most intense split band and the shoulders at 950 and 1115 cm^{-1} observed in the IR spectrum is thus in accordance with the existence of a small amount of at least one type of strong $[bmim]^+ - [BF_4]^-$ pair. However, the shoulder at 1115 cm^{-1} can also be related to the cation in-plane HCCH bending mode (calculated ~1130 cm^{-1}) (Fig. 4(a)). Thus, this IR region cannot discriminate between 'open' and 'closed' ion pairs, but can predict that most $[BF_4]^-$ in ILs exist in a symmetry lower than T_d.

One additional feature found in the calculated IR spectra of cation–anion pairs is the blue shift of the mode characteristic of out-of-plane ring NC(H)N CH bending vibrations. The IR mode at ~824 cm^{-1} calculated for the $[bmim(GA)]^+$ cation and corresponding to the experimental band at 848 cm^{-1} is shifted to ~916 and ~913 cm^{-1} for 'open' and 'closed' $[bmim(GA)]^+ - [BF_4]^-$ ion pairs, respectively (Fig. 4(b)). Also, the IR mode at ~748 cm^{-1} calculated for $[bmim(GA)]^+$ and corresponding to the experimental band at 754 cm^{-1} is red shifted to ~725 and ~730 cm^{-1} for 'open' and 'closed' $[bmim(GA)]^+ - [BF_4]^-$ pairs, respectively. This band is assigned to a mixture of out-of-plane HCCH and NC(H)N CH bending vibrations. Both of these features are probably related mainly to the F···H hydrogen bonds observed in the pair models. However, our experimental results indicate no similarly shifted bands.

High-wavenumber vibrations

Figure 5 shows the IR spectrum of [bmim][BF_4] and the computed spectra of $[bmim(GA)]^+$ and the $[bmim(GA)]^+ - [BF_4]^-$ pair models. The vibrational modes above 3100 cm^{-1} are assigned to ring C–H stretching vibrations, while modes lower than 3000 cm^{-1} originate from the alkyl chain. In the spectrum of [bmim][BF_4] there are two most intense bands at ~3120 and 3160 cm^{-1}, the former with a low wavenumber shoulder. However, the three computed IR modes characteristic of ring C–H stretching vibrations of $[bmim(GA)]^+$ cation are overlapping and only one broad band at 3185 cm^{-1} in the simulated spectrum is visible (Table 5, Fig. 5). For the ion pairs, the C_1–H_{11} force constant is reduced and the NC(H)N C–H stretching vibration is red-shifted yielding modes at 3162 and 3116 cm^{-1} for 'open' and 'closed' $[bmim(GA)]^+ - [BF_4]^-$ pairs, respectively. Also, it is important to note that the IR intensities of such modes in cation–anion pairs are at least 6 times stronger for the 'open' model (and 9 times for 'closed' model) compared to the corresponding band in the cation (Table 5). Therefore, the experimental IR modes at 3120 and 3160 cm^{-1} can be interpreted as quasi-diatomic NC(H)N C–H stretching vibrations of 'closed' and 'open' pairs, respectively. In addition, the low frequency shoulder at ~3100 cm^{-1} observed in the IR spectrum of [bmim][BF_4] can

DOI: 10.1002/jrs

JRS

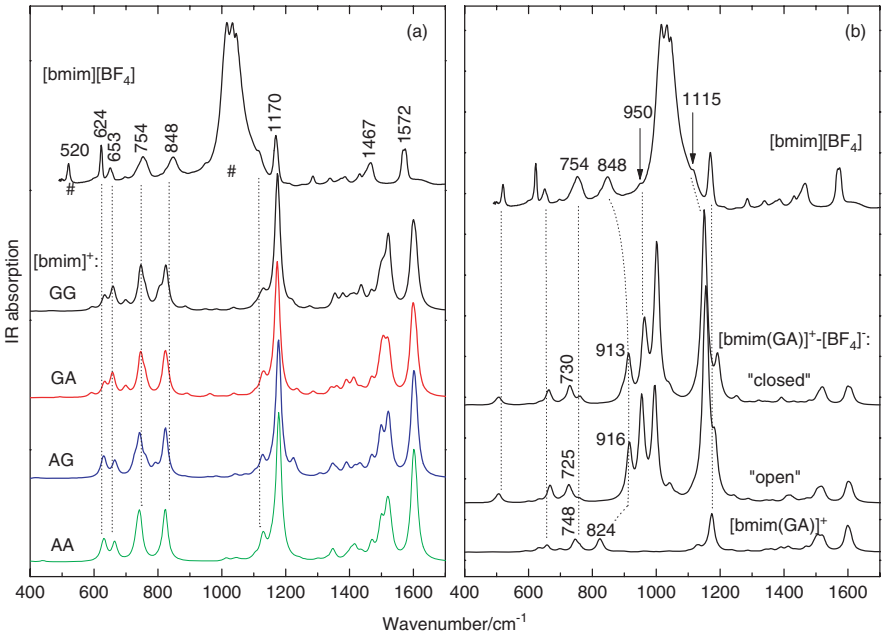

Figure 4. IR spectra of [bmim][BF_4] together with the computed IR spectra of $[bmim]^+$ conformers (a) and $[bmim(GA)]^+ - [BF_4]^-$ ion pairs (b) # indicates anion contribution. This figure is available in colour online at www.interscience.wiley.com/journal/jrs.

indicate the presence of an additional type of cation–anion pair (e.g. with opposite HCCH site for $[BF_4]^-$).

Detailed Raman spectroscopy study

Identification of bmim cation conformers

The calculated Raman spectra of different $[bmim]^+$ conformers and the experimental Raman spectrum of [bmim][BF_4] are shown in Fig. 6. As evident from Fig. 3(b) the region of 200–1200 cm^{-1} should be useful for identifying different $[bmim]^+$ conformers. Our tentative assignments of the calculated modes of $[bmim]^+$ conformers and their correlation with the experimental Raman spectrum of [bmim][BF_4] are found in Table 4. Earlier studies by Ozawa *et al*.[13] show that the Raman spectra of [bmim][Cl] and [bmim][Br] crystals can be very well reproduced by the calculated spectra of AA and GA $[bmim]^+$ conformers. They found two characteristic Raman bands of the [bmim][Cl] crystal at 625 and 730 cm^{-1} and three characteristic bands of the [bmim][Br] crystal at 500, 603, and 701 cm^{-1} to originate from the AA and GA forms, respectively. Also, it was suggested that the AA and GA cation conformers coexist in [bmim][BF_4].

According to our calculated and experimental Raman spectra in the 200–1200 cm^{-1} region at least four GG, GA, AG, and AA $[bmim]^+$ conformers exist in [bmim][BF_4] at room temperature. The calculated Raman spectra show that all of these conformers can contribute to the very intense 1023 cm^{-1} mode characteristic of ring $CH_2(N)$ and $CH_3(N)$ CN stretching vibrations, but that most other modes are not found for all conformers. As an example, the band observed at 325 cm^{-1} can be assigned to $CH_2(N)$, $CH_3(N)$ bending and CCCC deformational vibrations of both GA (calculated 325 cm^{-1})

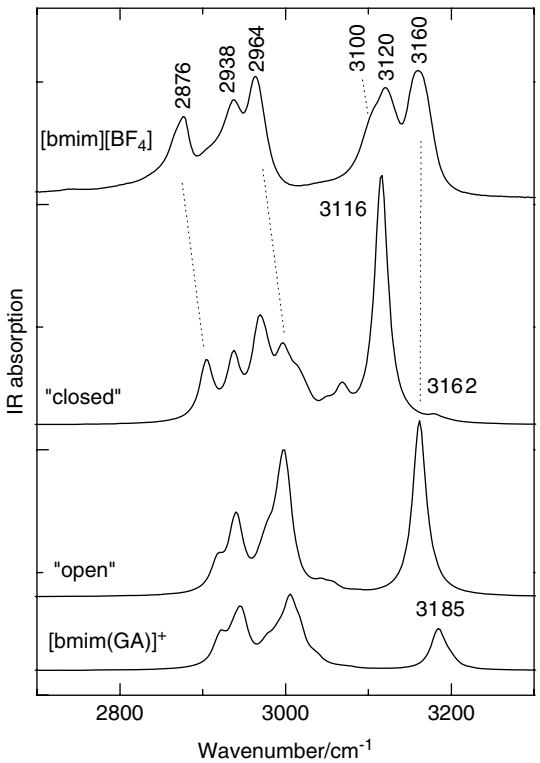

Figure 5. C–H stretching region of the IR spectrum of [bmim][BF_4] together with the computed spectra of 'closed' and 'open' $[bmim(GA)]^+ - [BF_4]^-$ ion pairs and the $[bmim(GA)]^+$ cation. The frequencies were corrected by an empirical scale factor 0.97.

DOI: 10.1002/jrs

Table 4. The correlation between experimental Raman modes of [bmim][BF_4] and the calculated Raman active modes of different $[bmim]^+$ conformers in the region 200–1200 cm^{-1}

[bmim]$^+$ conformers:				Tentative assignments	Exp. Raman[a]
GG	GA	AG	AA		
	325		316	b(CH_3(N), CH_2(N)), δ(CCCC)	325 m
			340	b(CH_3(N), CH_2(N)), b(CCCC)	352 w
		416		b(CH_3(N), CH_2(N), CH_3)	~413 w
594	592			b(ring o.o.pl.), $\nu_{i.ph.}$(CH_2(N), CH_3(N))	600 m
		627	626	b(ring o.o.pl.), $\nu_{i.ph.}$(CH_2(N), CH_3(N))	624 m
660	658	665	665	b(ring o.o.pl.), ν(CH_3(N))	~655 w
699	699			$\nu_{o.o.ph.}$(CH_2(N), CH_3(N))	700 w
			734	$\nu_{o.o.ph.}$(CH_2(N), CH_3(N))	~735 vw
804				ν_{sym}(chain CC), $b_{i.ph.}$(ring HCCH, NC(H)N o.o.pl.)	808 w
	822			$b_{i.ph.}$(ring HCCH, NC(H)N o.o.pl.), ν_{sym}(chain CC)	
	828			$b_{i.ph.}$(ring HCCH, NC(H)N o.o.pl.), ν_{sym}(chain CC)	825 m
		886		ν_{sym}(CH_2–CH_2–CH_3 CCC)	883 m
			919	ν_{sym}(CH_2–CH_2–CH_3 CCC)	905 m
949				$\nu_{o.o.ph.}$((N)CH_2–CH_2, CH_2–CH_3 CC)	~945 w
983		983		ν((N)CH_2–CH_2 CC)	975 m
1035	1037			ν(ring CN i.pl. i.ph., CH_2(N), CH_2–CH_3 CC)	1023 s
		1038	1038	ν(ring CN i.pl. i.ph., CH_3(N))	
1039				ν(ring CN i.pl. o.o.ph., CH_3(N))	
	1039			ν(ring CN i.pl. o.o.ph., CH_2(N), CH_3(N)), ν(CH_2–CH_3 CC)	
		1043	1044	ν(ring CN i.pl. o.o.ph., CH_2(N)), $\nu_{i.ph.}$((N)CH_2, CH_2, CH_3 CC)	
1079	1062	1073	1057	ν_{asym}(chain CCC)	1055 m
1104	1104	1104	1105	b((N)CH_3 CH), ν_{asym}(ring CN)	1092 m
1130		1128		ν(CH=CH CC)	
	1133			ν_{sym}(chain CCC), ν(CH=CH CC)	
			1133	ν_{sym}(chain CCC)	1117 m
	1152	1155		ν(chain CC), b(butyl CH)	1130 m (sh)

b, bending; δ, deformational; ν, stretching; sym and asym, symmetric and asymmetric vibrations, respectively; i.pl., in-plane; o.o.pl., out-of-plane; i.ph. and o.o.ph., in-phase and out-of-phase vibrations, respectively.

[a] Experimental Raman intensities (s: 0.5–1.0, m: 0.1–0.5, w: 0.05–0.1, vw: <0.05) were obtained from a spectrum normalized to the most intense band (1023 cm^{-1}).

Table 5. Calculated high-wavenumber C–H vibrational modes (ν, cm^{-1}), IR (I^{IR}, km/mol) and Raman (I^R, $Å^4$/a.m.u.) intensities of $[bmim(GA)]^+$, and $[bmim(GA)]^+ - [BF_4]^-$ 'closed' and 'open' ion pairs. The vibrational wavenumbers were corrected by an empirical scale factor 0.97

ν (GA)	I^{IR}	I^R	Assignments	ν 'open'	I^{IR}	I^R	ν 'closed'	I^{IR}	I^R	Assignments
3182	12.3	41.2	o.o.ph. HCCH	3162	149.3	43.5	3116	213.3	56.1	NC(H)N
3186	22.8	24.2	NC(H)N	3180	4.0	46.2	3181	4.1	46.7	o.o.ph. HCCH
3199	6.2	96.4	i.ph. HCCH + NC(H)N	3198	0.5	101.8	3199	0.9	98.8	i.ph. HCCH + NC(H)N

i.ph. and o.o.ph., in-phase and out-of-phase vibrations, respectively

and AA (calculated 316 cm^{-1}) conformers (Table 4). The corresponding mode of AG is shifted to 340 cm^{-1} and may be related with the band observed at 352 cm^{-1}. The GG conformer does not contribute in this region.

The 600–700 cm^{-1} region has four vibrational modes – each of them represents a group of two conformers. There are two (GG and GA) contributors to the bands at 600 and 700 cm^{-1} and two (AG and AA) contributors to the bands at 624 and 655 cm^{-1}. A simple conclusion is that the bands at 600 and 700 cm^{-1} are indicative of G conformers of C_7–C_8 and those at 624 and 655 cm^{-1} indicative of A conformers of C_7–C_8.

The presence of all the mentioned $[bmim]^+$ conformers in [bmim][BF_4] is first supported in the 800–950 cm^{-1} region.

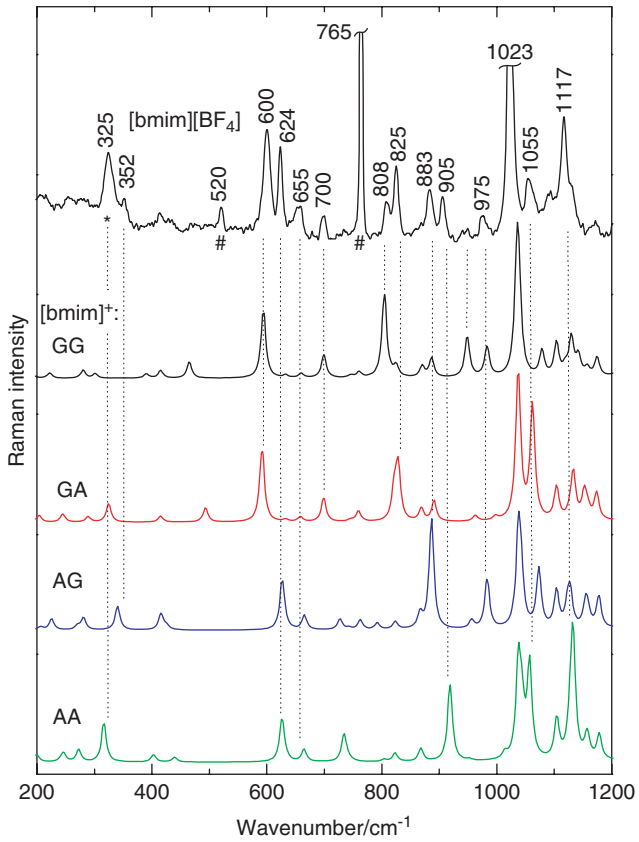

Figure 6. The Raman spectrum of [bmim][BF_4] and computed Raman spectra of [bmim]$^+$ conformers. # and * indicate anion bands and possible anion contribution, respectively. This figure is available in colour online at www.interscience.wiley.com/journal/jrs.

Here, four unique Raman bands are observed at 808, 825, 883, and 905 cm^{-1}, characteristic of combinations of ring HCCH, NC(H)N bending and alkyl chain CC stretching vibrations of GG (calculated 804 cm^{-1}), GA (822, 828 cm^{-1}), AG (886 cm^{-1}), and AA (919 cm^{-1}), respectively. Moving to higher wavenumbers, the band observed at 975 cm^{-1} can be correlated with the calculated modes at 983 cm^{-1} for both GG and AG, and thus the band is a sign of C_8–C_9 G conformer. The band at 1055 cm^{-1} correlates with the calculated modes at 1062 and 1057 cm^{-1} for GA and AA, respectively, and is thus a sign of C_8–C_9 A conformer. The asymmetry at the high wavenumber side of this peak may indicate a contribution from the AG conformer (calculated 1073 cm^{-1}) and in such a case, the 1055 cm^{-1} band is a sign of an A conformer in general. Finally, the intensity and sharpness of the band at 1117 cm^{-1} can be reproduced mainly by the AA conformer (calculated 1133 cm^{-1}), while all conformers can contribute to the broad base of this band.

Apart from the intense bands, even the small features observed in the 200–1200 cm^{-1} region can be explained using the [bmim]$^+$ conformers. Thus, the experimental features at 413, 735, and 945 cm^{-1} can be related with AG (calculated 416 cm^{-1}), AA (calculated 734 cm^{-1}) and GG (calculated 949 cm^{-1}), respectively.

Population of bmim cation conformers

Using the four characteristic modes in the experimental Raman spectrum and theoretical Raman spectra of different [bmim]$^+$ conformers, it is possible to estimate the population of each conformer.[10,35] By a Gaussian multipeak fitting procedure applied to the 780–920 cm^{-1} spectral region in the Raman spectrum of [bmim][BF_4] (Fig. 6) the relative amplitudes of the four vibrational modes were estimated. The ratios between these peak amplitudes (A_{ij}, i, j = A,G) were then corrected by the Raman cross-sections (σ_{ij}) using *ab initio* calculations and by the multiplicity m_{ij} to obtain the ratios between the populations of different [bmim]$^+$ conformers, n_{ij}/n_{ii}, and the relative fractions, n_{ij}:

$$\frac{n_{ij}}{n_{ii}} = \frac{A_{ii}}{A_{ij}}\frac{\sigma_{ij}}{\sigma_{ii}}\frac{m_{ij}}{m_{ii}}, \qquad i,j = \mathrm{A,G};$$

$$\sum_{i,j} n_{ij} = n_{\mathrm{AA}} + n_{\mathrm{GA}} + n_{\mathrm{AG}} + n_{\mathrm{GG}} = 1. \qquad (1)$$

The calculated ratios and estimated fractions (n_{ij}) of different [bmim]$^+$ conformers in IL at room temperature have been collected in Table 6. It is known, however, that the approach has some shortcomings; e.g. the Raman intensities are for each selected conformer in vacuo (i.e. condensed phase effects are neglected). But even if only approximate, the obtained results show that almost half of the cations in [bmim][BF_4] occupy a GA conformation state (fraction 0.48). However, there are some differences compared with the data presented in literature.[35] The fraction of anti (first anti in our terminology) was there estimated to be 0.58 or 0.65 (Raman peak-area or peak-height). By summarizing

Table 6. Relative populations (n_{ij}) of different [bmim]$^+$ conformers in [bmim][BF_4] estimated using Raman spectroscopy and *ab initio* calculations

A_{ij}/A_{ii}		n_{ij}/n_{ii}		n_{ij}	
$A_{\mathrm{GA}}/A_{\mathrm{AA}}$	1.83	$n_{\mathrm{GA}}/n_{\mathrm{AA}}$	1.67	n_{GA}	0.48
$A_{\mathrm{AG}}/A_{\mathrm{AA}}$	1.74	$n_{\mathrm{AG}}/n_{\mathrm{AA}}$	0.61	n_{AG}	0.17
$A_{\mathrm{GG}}/A_{\mathrm{AA}}$	1.03	$n_{\mathrm{GG}}/n_{\mathrm{AA}}$	0.23	n_{GG}	0.07
				n_{AA}	0.28

A_{ij}, A_{ii} – the amplitudes of peaks characteristic of different [bmim]$^+$ conformers (GG – 808 cm^{-1}, GA – 825 cm^{-1}, AG – 883 cm^{-1}, AA – 905 cm^{-1});
n_{ij}/n_{ii} – the ratios between the populations of different conformers: the following multiplicities of [bmim]$^+$ conformers: AA – 1, GA – 2 ($G^{(+)}A$, $G^{(-)}A$), AG – 2 ($AG^{(+)}$, $AG^{(-)}$), GG – 4 ($G^{(+)}G^{(+)}$, $G^{(-)}G^{(-)}$, $G^{(+)}G^{(-)}$, $G^{(-)}G^{(+)}$) and Raman mode intensities calculated *ab initio* (supporting information): GG – 804.4 cm^{-1}, GA – averaged of 821.5 and 828.3 cm^{-1} modes, AG – 886.4 cm^{-1}, AA – 918.8 cm^{-1}, were used.

populations of $[bmim]^+$ conformers ($n_{AA} + n_{AG}$) our fraction is only 0.45. However, this is closer to the A fraction estimated by Canongia Lopes *et al*.[35] from the distribution of dihedral angles of cations in $[bmim][BF_4]$ (0.40 and 0.38 for the small and large MD simulation boxes, respectively). The population of AG and GG conformers was found to be 0.17 and 0.08, respectively, consistent with the calculated energies – both the AG and GG are high-energy conformers.

Identification of cation–anion pairs

As can be seen from Fig. 7(a) the calculated Raman spectra of the $[bmim(GA)]^+$ cation and the $[bmim(GA)]^+ - [BF_4]^-$ ion pairs are very similar in the 400–1200 cm^{-1} region (apart from the $[BF_4]^-$ modes). However, in the 1200–1600 cm^{-1} region, small differences in mode intensities between the various models can be observed. Also in the high wavenumber region of alkyl chain C–H stretching vibrations (below 3100 cm^{-1}), minor differences connected mainly with red shifts of modes due to cation–anion pairs can be observed (Fig. 7(b)). A larger red shift of these modes in the 'open' cation–anion model compared with the 'closed' model may be connected with increased cation–anion interactions. However, clear assignments (i.e. 'open' and 'closed' models) of the Raman modes in this spectral region cannot be made. Additionally, a similar red shift as was detected by IR spectroscopy for the modes characteristic of ring C–H stretches (above 3100 cm^{-1}) is here found for the broad band at 3112 cm^{-1}, probably shifted from the likewise broad band centerd at 3174 cm^{-1}. The calculated modes corresponding to the 3174 cm^{-1} experimental peak are found as doublets, very similar for cation and cation–anion pairs (Table 5), while the lower very broad band with maximum at ~3112 cm^{-1} is probably due to the calculated modes at 3162 and 3116 cm^{-1} of 'open' and 'closed' ion pairs, respectively. The latter two bands are also found to have a strong IR intensity.

DSC and temperature-dependent Raman spectroscopy studies

In order to determine the most stable $[bmim]^+$ conformer, a Raman temperature study was undertaken. However, first a calorimetric study must be made to ensure that a temperature interval can be chosen such that no phase transition disturbs the measurement. A melting point of 198.2 K and a degradation temperature of 680 K have previously been reported for $[bmim][BF_4]$.[5] No features characteristic of the formation of crystalline domains in $[bmim][BF_4]$ were found in the entire DSC trace (Fig. 8). The glass transition temperature (T_g) was found to be 189.7 K (−83.5 °C). Thus, we could safely perform a Raman temperature study in the interval 210–650 K. However, an upper limit of 448 K was chosen for practical reasons.

As discussed above in the Raman section, the 800–950 cm^{-1} region contains four bands at 808, 825, 883, and 905 cm^{-1} characteristic of the GG, GA, AG, and AA $[bmim]^+$ conformers, respectively. Using these unique bands temperature-dependent Raman spectroscopy was used to probe the concentration changes of the $[bmim]^+$ conformers in $[bmim][BF_4]$.

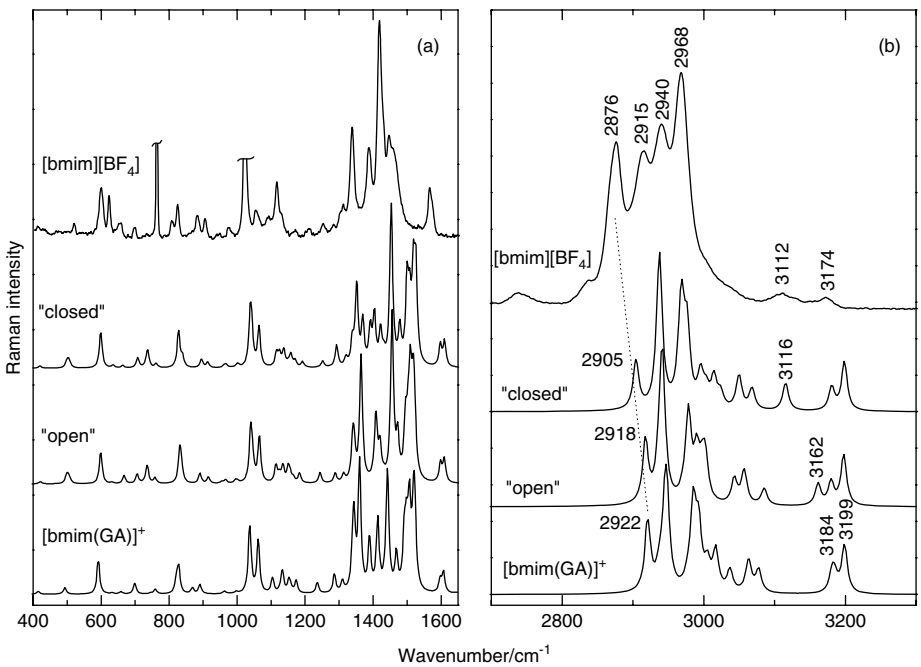

Figure 7. Selected 400–1600 cm^{-1} (a) and high frequency (b) regions in the Raman spectrum of the $[bmim][BF_4]$ ionic liquid, and the computed spectra of 'closed' and 'open' $[bmim(GA)]^+ - [BF_4]^-$ ion pairs, and the $[bmim(GA)]^+$ cation. In 7(b), frequencies were corrected by an empirical scale factor 0.97.

DOI: 10.1002/jrs

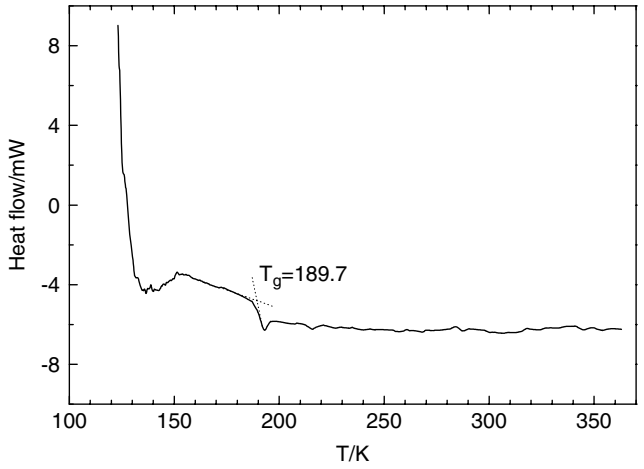

Figure 8. DSC trace for [bmim][BF_4].

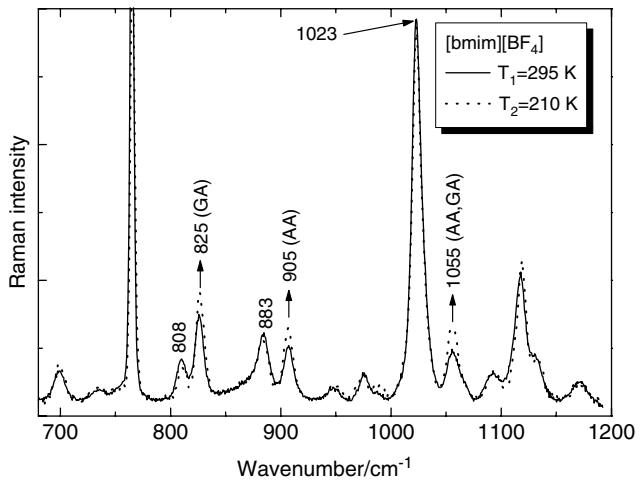

Figure 9. Temperature-dependent Raman spectra of [bmim][BF_4]. The spectra have been normalized to the 1023 cm^{-1} mode.

No significant changes were possible to detect on heating the sample from ~295 (room temperature) to 348 K, and on increasing the temperature further to 448 K, only a negligibly small decrease in the intensity of the 825 cm^{-1} band was detected (not shown). However, when decreasing the temperature from ~295 to 210 K, differences in the Raman spectra were clearly observed (Fig. 9). The intensity, normalized using the 1023 cm^{-1} band, of the modes at 825, 905, and 1055 cm^{-1} characteristic of the two most stable conformers of [bmim]$^+$: GA and AA, clearly increase in the low temperature spectrum. Thus, the computed stability of these conformers is further supported experimentally.

CONCLUSIONS

We have shown that the conformational isomerism of [bmim]$^+$ in the [bmim][BF_4] IL can be studied in detail using a combination of vibrational spectroscopy and first-principle calculations. Especially, Raman spectroscopy has proven the existence of unique [bmim]$^+$ conformers.

The presence of four [bmim]$^+$ conformers at room-temperature was firmly established by four unique Raman modes at 808, 825, 883, 905 cm^{-1} characteristic of the GG, GA, AG, and AA conformers, respectively. The estimated fractions of conformers were found to be 0.48, 0.28, 0.17, and 0.07 for GA, AA, AG, and GG, respectively. Furthermore, the temperature-dependent Raman studies result in increasing intensities with decreasing temperature for modes due to the computationally most stable conformers, AA (0) and GA (+2.36 kJ mol^{-1}).

Taking also the cation–anion interactions into account via [bmim]$^+$ – [BF_4]$^-$ ion pairs, it is possible to explain the structural origin of the broad B–F stretching vibrations and the features in the high-wavenumber region of ring C–H stretching vibrations observed in the IR and Raman spectra. Thus the IL is considered to be a mix of cation conformers as well as a mix of ion pairs. The ion pairs do bring a strong improvement compared to the use of only the free ions as models but, in future, it will be important to consider more realistic models involving ionic clusters for a better representation of the IL local electric field and H-bond network.

Supplementary material

Supplementary electronic material for this paper is available in Wiley InterScience at: http://www.interscience.wiley.com/jpages/0377-0486/suppmat/

Acknowledgements

The authors are grateful to Assistant Prof. Alexander Matic for his stimulating discussions and to Dr Ezio Zanghellini for his technical assistance. R.H acknowledges a scholarship from the Swedish Institute. They gratefully acknowledge the financial support from the FUTURA foundation and the Swedish Research Council. The calculations have mainly been carried out at the Center for Parallel Computers (PDC) and the National Supercomputer Centre (NSC) through a grant from the Swedish National Allocations Committee (SNAC).

REFERENCES

1. Angell CA, Xu W, Yoshizawa M, Belieres J-P. Ionic liquids: inorganic vs organic, protic vs aprotic, and Coulomb control vs van der Waals control. *International Symposium on Ionic Liquids in Honour of Marcelle Gaune-Escard*, Carry le Rouet, 2003; 389.
2. Blanchard LA, Hancu D, Beckman EJ, Brennecke JF. *Nature* 1999; **399**: 28.
3. Welton T. *Chem. Rev.* 1999; **99**: 2071.
4. Ito Y, Nohira T. *Electrochim. Acta* 2000; **45**: 2611.
5. Wu B, Reddy RG, Rogers RD. *Proceedings of Solar Forum 2001. Solar Energy: The Power to Choose*. ASME: Washington, DC, April 21–25, 2001.
6. Branco Luís C, Rosa João N, Moura Ramos Joaquim J, Afonso Carlos AM. *Chem. Eur. J.* 2002; **8**: 3671.
7. Forsyth SA, Pringle JM, MacFarlane DR. *Aust. J. Chem.* 2004; **57**: 113.
8. Turner EA, Pye CC, Singer RD. *J. Phys. Chem. A* 2003; **107**: 2277.

9. Umebayashi Y, Fujimori T, Sukizaki T, Asada M, Fujii K, Kanzaki R, Ishiguro S. *J. Phys. Chem. A* 2005; **109**: 8976.
10. Lassègues JC, Grondin J, Holomb R, Johansson P. *J. Raman Spectrosc.* 2007; **38**: 551.
11. Hayashi S, Ozawa R, Hamaguchi H. *Chem. Lett.* 2003; **32**: 498.
12. Holbrey JD, Reichert WM, Nieuwenhuyzen M, Johnson S, Seddon KR, Rogers RD. *Chem. Commun.* 2003; **14**: 1636.
13. Ozawa R, Hayashi S, Saha S, Kobayashi A, Hamaguchi H. *Chem. Lett.* 2003; **32**: 948.
14. Berg RW, Deetlefs M, Seddon KR, Shim I, Thompson JM. *J. Phys. Chem. B* 2005; **109**: 19025.
15. Katayanagi H, Hayashi S, Hamaguchi H, Nishikawa K. *Chem. Phys. Lett.* 2004; **392**: 460.
16. Heimer NE, Del Sesto RE, Meng Z, Wilkes JS, Carper WR. *J. Mol. Liq.* 2006; **124**: 84.
17. Katsyuba SA, Zvereva EE, Vidiš A, Dyson PJ. *J. Phys. Chem. A* 2007; **111**: 352.
18. http://www.merck.de (Merck KGaA, Darmstadt, Germany).
19. Frisch MJ, Trucks GW, Schlegel HB, Scuseria GE, Robb MA, Cheeseman JR, Montgomery JA, Jr, Vreven T, Kudin KN, Burant JC, Millam JM, Iyengar SS, Tomasi J, Barone V, Mennucci B, Cossi M, Scalmani G, Rega N, Petersson GA, Nakatsuji H, Hada M, Ehara M, Toyota K, Fukuda R, Hasegawa J, Ishida M, Nakajima T, Honda Y, Kitao O, Nakai H, Klene M, Li X, Knox JE, Hratchian HP, Cross JB, Bakken V, Adamo C, Jaramillo J, Gomperts R, Stratmann RE, Yazyev O, Austin AJ, Cammi R, Pomelli C, Ochterski JW, Ayala PY, Morokuma K, Voth GA, Salvador P, Dannenberg JJ, Zakrzewski VG, Dapprich S, Daniels AD, Strain MC, Farkas O, Malick DK, Rabuck AD, Raghavachari K, Foresman JB, Ortiz JV, Cui Q, Baboul AG, Clifford S, Cioslowski J, Stefanov BB, Liu G, Liashenko A, Piskorz P, Komaromi I, Martin RL, Fox DJ, Keith T, Al-Laham MA, Peng CY, Nanayakkara A, Challacombe M, Gill PMW, Johnson B, Chen W, Wong MW, Gonzalez C, Pople JA. *Gaussian 03, Revision D.01*, Gaussian, Inc.: Wallingford CT, 2004.
20. Becke AD. *Phys. Rev. A* 1998; **38**: 3098.
21. Lee C, Yang W, Parr RG. *Phys. Rev. B* 1998; **37**: 785.
22. Rassolov VA, Pople JA, Ratner MA, Windus TL. *J. Chem. Phys.* 1998; **109**: 1223.
23. Breneman CM, Wiberg KB. *J. Comput. Chem.* 1990; **11**: 361.
24. Monev V, Spassova M, Champagne B. *Int. J. Quantum Chem.* 2005; **104**: 354.
25. Meng Z, Dölle A, Carper WR. *J. Mol. Struct. (Theochem)* 2002; **585**: 119.
26. Talaty ER, Raja S, Storhaug VJ, Dölle A, Carper WR. *J. Phys. Chem. B* 2004; **108**: 13177.
27. Tsuzuki S, Tokuda H, Hayamizu K, Watanabe M. *J. Phys. Chem. B* 2005; **109**: 16474.
28. Dong K, Zhang S, Wang D, Yao X. *J. Phys. Chem. A* 2006; **110**: 9775.
29. Köddermann T, Wertz K, Heintz A, Ludwig R. *ChemPhysChem* 2006; **7**: 1944.
30. Shigeto S, Hamaguchi H. *Chem. Phys. Lett.* 2006; **427**: 329.
31. Wang Y, Li H, Han S. *J. Chem. Phys.* 2005; **123**: 174501.
32. Dymek CJ, Stewart JJP Jr. *J. Inorg. Chem.* 1989; **28**: 1472.
33. Liu Z, Huang S, Wang W. *J. Phys. Chem. B* 2004; **108**: 12978.
34. Katsyuba SA, Dyson PJ, Vandyukova EE, Chernova AV, Vidiš A. *Helv. Chim. Acta* 2004; **87**: 2556.
35. Canongia Lopes JNA, Pádua AAH. *J. Phys. Chem. B* 2006; **110**: 7485.